Seismic Resilience of Aging Bridges and Evolving Road Networks

Fabio Biondini, Luca Capacci, and Andrea Titi
fabio.biondini@polimi.it, luca.capacci@polimi.it, andrea.titi@polimi.it
Department of Civil and Environmental Engineering, Politecnico di Milano, Milano, Italy

Abstract: This paper investigates the seismic resilience of aging infrastructures and presents a probabilistic approach to life-cycle seismic assessment of concrete bridges exposed to corrosion and resilience analysis of evolving road networks under prescribed earthquake scenarios. The seismic demand is evaluated for each bridge in the network based on a ground motion prediction equation in terms of earthquake magnitude and epicentral distance. The corresponding levels of seismic damage are derived from the bridge time-variant fragilities and related to vehicle restrictions and traffic limitations. Finally, a traffic analysis of the road network is carried out to compute both the time-variant system functionality and life-cycle seismic resilience under prescribed post-event recovery processes considering the evolution over time of the road network.

Keywords: Seismic resilience, aging bridges, evolving road networks, earthquake scenarios.

Introduction

Planning proper road management strategies is a key task to satisfy the fundamental needs of the communities not only under full operational conditions, but also in a state of emergency. In particular, highway bridges are essential to guarantee suitable functionality levels in the aftermath of an extreme event, such as an earthquake (Chang 2009) in order to ensure both a quick deployment of aids and resources to distressed communities and a prompt repair of the surrounding lifelines and buildings (Carturan 2013). In addition, to fulfill the requirements of appropriate performance levels during the operational state, road management policy has to be faced with the compliance of old roads, mainly constructed in the 50's or 60's, to new construction standards and traffic needs (Papageorgiou *et al*. 2012).

Therefore, the definition of effective post-event recovery processes of damaged bridges and adequate retrofit interventions, also considering an upgrade of the existing network, are important factors to ensure suitable resilience levels of the entire infrastructure (Venkittaram and Banerjee 2014). Resilience can be defined as the capability of a system to withstand the effects of disruptive events and to recover promptly and efficiently the pre-event functionality (Bruneau *et al*. 2003, Cimellaro *et al*. 2010, Decò *et al*. 2013). This indicator has recently gained a prominent importance in design and assessment of structures and infrastructure systems, particularly with reference to potential damage and disruption caused by sudden extreme events such as earthquakes (Chang and Shinozuka 2004, Bruneau and Reinhorn 2007, Biondini *et al*. 2015b).

However, for aging systems, progressive damage can also arise continuously over time due to the effects of structural deterioration, which can reduce the bridge structural performance, the network functionality and, consequently, the system resilience. Consequently, seismic resilience of deteriorating bridges and infrastructure networks depends on the time of occurrence of the seismic event (Titi and Biondini 2013, Biondini *et al*. 2015a, 2016, Titi *et al*. 2015). Therefore, system functionality and seismic resilience should be formulated as time-variant performance indicators under a life-cycle perspective to properly support the decision making process and the definition of robust policies for life-cycle management of critical structures and infrastructure networks.

This paper presents a life-cycle probabilistic framework for seismic assessment of bridge structures and resilience analysis of road networks considering the interaction of environmental and seismic hazards under prescribed earthquake scenarios (Biondini *et al*. 2017). The proposed framework allows to incorporate the upgrade of existing networks to simulate system management interventions carried out at predefined time instants and to study the effects on the life-cycle network resilience. This approach is applied to reinforced concrete (RC) bridges in a highway network with detour and re-entry link. The bridges are exposed to chloride-induced corrosion and earthquake scenarios with different magnitude and epicenter location. The results show the effectiveness of the proposed framework to assess both the detrimental effects of aging and structural deterioration and the beneficial effects of a network upgrading relating the structural performance of bridges and the seismic resilience of road network.

Seismic Assessment of Spatially Distributed RC Bridges under Corrosion

Seismic assessment of RC bridges

In this study the seismic capacity of RC bridges under uncertainty is evaluated through probabilistic nonlinear incremental dynamic analysis (IDA, Vamvatsikos and Cornell 2002) by assuming the peak ground acceleration (PGA) as seismic intensity measure and the maximum drift $\theta_{max}=\Delta_{max}/H$, with Δ_{max} = maximum top displacement of a bridge pier and H = pier height, as damage measure.

The nonlinear behavior of the plastic hinges is defined in terms of bending moment versus curvature relationship based on the Mander model for concrete (Mander *et al*. 1988) and a bilinear elastic-plastic model for reinforcing steel. The hysteretic behavior is based on the Takeda model (Takeda *et al*. 1970), with a backbone curve defined by a stepwise linearization of the moment versus curvature diagram. The length of the plastic hinge is evaluated as proposed by Paulay and Priestley (1992).

Damage limitation and seismic fragility

Damage limit states are associated with the following threshold values of the maximum drift θ_{max} (Capacci 2015):

- Slight Damage (SD): $\theta_{max}=\theta_y$;
- Moderate Damage (MD): $\theta_{max}=\theta_y+0.3\theta_p$;
- Extensive Damage (ED): $\theta_{max}=\theta_y+0.6\theta_p$;

where $\theta_p=\theta_u-\theta_y$, and θ_y and θ_u are the drift values associated with, respectively, the first yielding and ultimate curvatures of the bridge piers in the undamaged state. In addition, a structural collapse limit state (SC), associated with the loss of dynamic equilibrium under ground motion, is considered.

The seismic capacity associated with the damage limit states under uncertainty are hence investigated through fragility curves, which are time-variant due to aging and structural deterioration (Biondini *et al*. 2016, 2017).

Effects of reinforcing steel corrosion

The application presented in this paper deals with RC bridges exposed to chloride-induced corrosion. The chloride propagation is modeled by the Fick's laws of diffusion and described by using cellular automata (Biondini *et al*. 2004). The main effect of the corrosion process is a reduction of the cross-sectional area of reinforcing steel bars (Bertolini *et al*. 2004). This effect can be described by means of a dimensionless damage index δ_s which provides a measure of damage within the range [0,1]. Corrosion may also cause a significant reduction of ductility of the reinforcing steel bars. Moreover, the formation of oxidation products may lead to propagation of longitudinal splitting cracks and concrete cover spalling. These effects are modeled as a reduction of both the ultimate steel strain ε_{su} and concrete cover strength f_c as a function of the damage index δ_s, as proposed in (Biondini and Vergani 2015). The corrosion rate at point $\mathbf{x}$ and time t depends on the chloride concentration $C=C(\mathbf{x}, t)$, and damage initiates once concentration reaches a critical value $C=C_{crit}$. Based on available data for chloride attacks, a linear relationship between corrosion rate and chloride concentration is assumed:

$$\frac{\partial \delta_s(t)}{\partial t} = q_s\, C(\mathbf{x},t) \tag{1}$$

where q_s is a damage rate coefficient. Further details on the corrosion model can be found in (Biondini *et al*. 2004).

Earthquake scenario and seismic demand

The seismic demand is evaluated based on the ground motion prediction equation proposed by Bindi *et al*. (2011):

$$\log_{10}\mathrm{PGA} = 3.672 + F_D(d,M) + F_M(M) + F_S + F_{sof} \tag{2}$$

$$F_D(d,M) = [-1.940 + 0.413\,(M - M_{ref})]\log_{10}\frac{\sqrt{d^2+h^2}}{d_{ref}} + -0.000134\left(\sqrt{d^2+h^2} - d_{ref}\right) \tag{3}$$

$$F_M(M) = \begin{cases} -0.262(M-M_h) - 0.0707(M-M_h)^2 & , M \le M_h \\ 0 & M > M_h \end{cases} \tag{4}$$

where the peak ground acceleration (PGA) is given in in cm/s^2, $F_D(d,M)$, $F_M(M)$, F_S, and F_{sof} are the distance function, the magnitude scaling, the site amplification, and the style-of-faulting correction, respectively, M is the moment magnitude, d is the epicentral distance (in km), h=10.322 km is a pseudo-depth parameter, d_{ref}=1 km, M_{ref}=5, and M_h=6.75.

Seismic Resilience of Road Networks

Network traffic flow analysis

The performance and functionality of road networks can be assessed based on traffic flow response and minimum travel time (Bocchini and Frangopol 2011). The travel time c_{ij} of the arc *i-j* can be expressed as a function of several parameters:

$$c_{ij} = c_{ij}(f_{ij}, \mathbf{p}_{\mathbf{road}}, \mathbf{c}_{\mathbf{road}}) \tag{5}$$

where f_{ij} is the vehicle flow per unit of time in the arc *i-j*, $\mathbf{p}_{\mathbf{road}}$ includes road parameters such as arc length L_{ij} and number of lanes n_L, and $\mathbf{c}_{\mathbf{road}}$ is the road class depending on several factors, including the minimum distance d_{min} between vehicles, the corresponding speed limit, or critical speed v_{cr}, and the maximum

speed limit $v_{\max}$. The travel time c_{ij} is related to the traffic flow f_{ij} as follows:

$$c_{ij} = c_{ij}^0 \left[1 + \alpha \left(\frac{f_{ij}}{f_{ij}^{cr}} \right)^{\beta} \right] \tag{6}$$

where $c^0_{ij}=L_{ij}/v_{\max}$ is the travel time at free flow, $f_{ij}^{cr}=n_L(v_{cr}/d_{\min})$ is the practical capacity, α=0.15, and β=4 (Martin and McGuckin 1998). The total travel time *TTT* is evaluated according to Bocchini and Frangopol (2011):

$$TTT = \sum_{i \in I} \sum_{j \in J} \int_0^{f_{ij}} c_{ij}(f)\, df \tag{7}$$

where i and j are generic nodes of the network, and I and J are the whole sets of nodes. The optimal traffic flow distribution is identified by minimizing the total travel time. In this study, initial traffic flows are prescribed a priori.

Type of users and traffic limitations

Three different types of users are considered: light vehicles f_l, heavy vehicles f_h, and emergency vehicles f_e. Restrictions to each type of vehicle and limitations to road traffic capacity are applied depending on the damage state of the bridges in the network (Mackie and Stojadinović 2006). Four traffic limitations, identified by a Decision Variable $DV_b=k$ associated to four bridge damage levels k=1,...,4, are assumed:

- Weight Restriction (DV_b=1): transit of heavy vehicles is forbidden and maximum speed along the bridge is reduced;
- One Lane Open Only (DV_b=2): only one lane is left open to traffic due to repair activities;
- Emergency Access Only (DV_b=3): transit of emergency vehicles only is allowed;
- Closure (DV_b=4): transit is forbidden to all vehicles.

These traffic limitations are represented as follows:

$$\begin{cases} f_h = 0 \text{ and } \tilde{v}_{\max} < v_{\max} & , DV_b = 1 \\ n_L = 1 & , DV_b = 2 \\ f_l = 0 & , DV_b = 3 \\ f_e = 0 \text{ or } n_L = 0 & , DV_b = 4 \end{cases} \tag{8}$$

More details can be found in Capacci (2015) and Biondini *et al*. (2015b).

Network functionality and recovery model

The functionality $Q=Q(t)\in[0,1]$ of the road network is defined as follows (Bocchini and Frangopol 2012):

$$Q(t) = \frac{TTT_u}{TTT_d(t)} \tag{9}$$

where TTT_u and $TTT_d=TTT_d(t)$ are the total travel times of the undamaged and damaged network at time t, respectively. A seismic event that strikes the system at time t_0 may cause a sudden loss of functionality $\Delta Q=\Delta Q(t_0)$ due to vehicle restrictions and traffic limitations imposed to damaged bridges.

Post-event repair activities lead to progressive restoration of the functionality drop ΔQ over a recovery time interval $\delta_r = t_f - t_i$, where $t_i = t_0+\delta_i$ and t_f are the initial and final time of the restoration process, respectively, and δ_i is the idle time between the time of occurrence t_0 and the repair initiation t_i. The following recovery model $r=r(t)\in[0,1]$ is adopted at the bridge component level (Titi *et al*. 2015):

$$r(\tau) = \begin{cases} \omega^{1-\rho}\tau^{\rho} & , 0 \le \tau \le \omega \\ 1-(1-\omega)^{1-\rho}(1-\tau)^{\rho} & , \omega < \tau \le 1 \end{cases} \tag{10}$$

where $\tau=(t-t_i)/\delta_r\in[0,1]$ is a dimensionless time variable, and $\omega\in[0,1]$ and $\rho\ge0$ are parameters which define the shape of the recovery profile. The values of the shape parameters depend on the damage state to be restored. The road network functionality is described by a discrete set of values as a function of the damage state of the bridges, evolving from the initial damage to the fully restored state. Therefore, at the network level a constant stepwise recovery model is achieved (Padgett and DesRoches 2007).

Network seismic resilience

The seismic resilience R of the road network is computed as follows:

$$R(t_0) = \frac{1}{t_h - t_0} \sum\nolimits_{\Delta t_{b,i}} Q_{\Delta t_{b,i}} \Delta t_{b,i} \tag{11}$$

where t_h is a time horizon and $Q_{\Delta tb,i}$ is the level of network functionality over the time interval $\Delta t_{b,i}$ between two subsequent steps of the restoration process, which depends on the damage states and corresponding repair activities carried out on the bridges in the network.

The seismic resilience can be computed for each damage state scenario resulting from the damage state of each bridge in the network. An overall indicator of network resilience versus the seismic demand is achieved by a weighted average of the resilience levels by assuming the damage probabilities as weight coefficients.

It is worth noting that the seismic resilience $R=R(t_0)$ is a function of the time of occurrence of the seismic event t_0 due to the combined effects of sudden seismic damage and continuous structural deterioration due to reinforcing steel corrosion, which affect both the functionality drop and the recovery profile (Biondini *et al*. 2015a).

Illustrative Example

RC box-girder bridge

The four-span continuous RC bridge shown in Figure 1 is considered (Biondini *et al*. 2015b, Titi *et al*. 2015). The total length of the bridge deck is 200 m, with spans of 50 m. The height of the bridge piers is 14 m. Figure 2a shows the box girder cross-section of the deck. The piers have circular cross-section (Mander *et al*. 2007) and are reinforced with 36 steel bars with diameter Ø=30 mm, as shown in Figure 2b. The constitutive laws of the materials are defined by the following initial nominal values of the material properties: concrete compression strength f_c=40 MPa; steel yielding strength f_{sy}=450 MPa; concrete ultimate strain in compression ε_{cu}=0.35%; steel ultimate strain ε_{su}=7.5%. Seismic analysis is carried out by considering a uniform gravity load of 315 kN/m, including self-weight, dead loads and a 20% of live loads, applied on the deck.

The deck is modeled by elastic beam elements, since nonlinear behavior is expected to develop only in the piers. Non-linear time-history dynamic analyses are performed for a set of 10 artificial earthquakes generated to comply with the elastic response spectrum given by Eurocode 8 for soil type B (SIMQKE 1976, CEN-EN 1998).

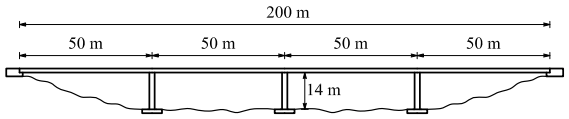

Figure 1. Four-span continuous RC bridge.

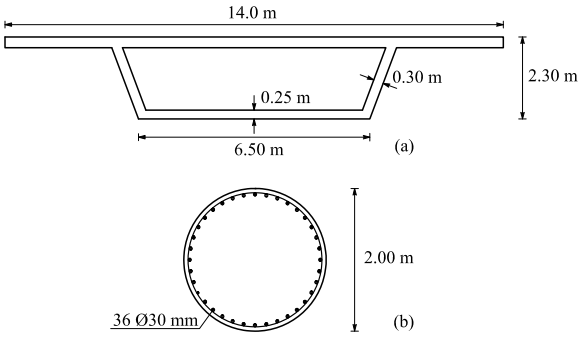

Figure 2. RC bridge: (a) deck cross-section; (b) pier cross-section, with reinforcement layout.

Probabilistic model and lifetime seismic capacities of the bridges

The piers are exposed to a chloride diffusive attack on the external surface, with nominal concentration C_0=3% [wt.%/c]. A nominal diffusivity coefficient D=15.8×10^{-12} m^2/sec is assumed. The corrosion damage is evaluated by assuming a nominal damage rate coefficient q_s = (0.02 year^{-1})/C_0, with corrosion initiation associated with a nominal critical threshold of concentration C_{crit}=0.6% [wt.%/c].

The uncertainties related to the structural system and the damage process are taken into account in probabilistic terms by assuming the random variables, probability distributions, and coefficients of variation listed in Table 1 (Biondini *et al*. 2006, Dolšek 2009). Nominal values are assumed as mean values. Random variables are considered uncorrelated. The fragility analysis is carried out by Monte Carlo simulation based on Latin Hypercube Sampling. Further details can be found in Biondini *et al*. (2016, 2017).

Table 1. Probabilistic model.

Random Variable (t = 0)	Type	C.o.V.
Concrete strength, f_c	Lognormal	5MPa/$f_{c,nom}$
Steel strength, f_{sy}	Lognormal	30MPa/$f_{sy,nom}$
Viscous damping, ξ	Normal (*)	0.40
Diffusivity, D	Normal (*)	0.20
Damage rate, q_s	Normal (*)	0.30
Chloride concentration, C_0	Normal (*)	0.30
Critical concentration, C_{crit}	Beta (**)	0.15

(*) Truncated distributions with non-negative outcomes.
(**) Lower bound b_{min} = 0.2; Upper bound b_{max} = 2.0.

Highway network and resilience level

Figure 3 shows the road network investigated. The network layout includes one origin and one destination, two identical bridges B_1 and B_2 located on the main highway close to the origin/destination nodes, and a detour route with a re-entry link.

The road network N2 (Figure 3.b) is an upgrade of the network N1 (Figure 3.a) that consists of an additional highway branch with a further bridge B_3, identical to bridges B_1 and B_2. The new highway branch allows for an additional and faster detour when bridges B_1 and B_2 are damaged. Table 2 summarizes the traffic parameters of each road segment (main highways, secondary road, re-entry link), including the road length L, the number of lanes n_L, the maximum speed v_{max}, the minimum speed v_{min}, the critical speed v_{cr}, and the minimum distance between vehicles d_{min}.

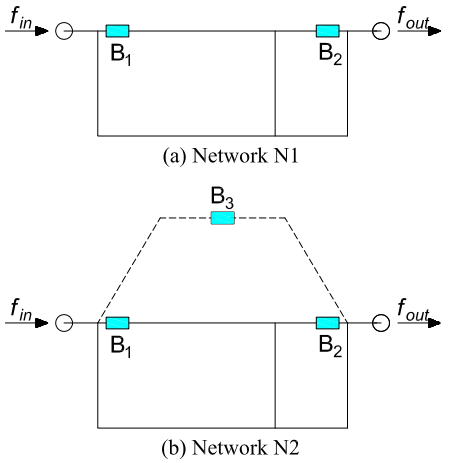

Figure 3. Highway networks: (a) existing network N1; (b) upgraded network N2.

Table 2. Traffic parameters of the road segments.

Traffic Parameters	L [km]	n_L	v_{max} [km/h]	v_{min} [km/h]	v_{cr} [km/h]	d_{min} [m/cars]
Highway Road	10	3	130	70	65	30
Secondary Road	40	2	90	50	65	30
Re-entry Link	1	1	90	50	65	30
New Highway	15	3	130	70	65	30

Traffic restrictions are applied to the bridges depending on their damage state. The loss of network functionality is recovered by post-event bridge repairs, which allow for a progressive removal of traffic limitations. The shape parameters ω and ρ of the bridge recovery profiles are selected based on the damage state to be restored. For each initial damage state k, stepwise partial increments of the network functionality at time instants t_p (where p=1,…,k) are obtained when the bridge seismic capacity reaches the target levels $r_{DS,p}$ over the given total recovery time interval δ_r. Shape parameters, capacity targets, and recovery time interval δ_r for the case study are listed in Table 3.

Table 3. Shape parameters, capacity targets, and recovery time intervals for each damage state.

Damage	ω	ρ	$r_{DS,1}$	$r_{DS,2}$	$r_{DS,3}$	$r_{DS,4}$	δ_r [days]
SD	0.20	2.0	1.00	-	-	-	30
MD	0.40	3.0	0.50	1.00	-	-	90
ED	0.60	4.0	0.20	0.50	1.00	-	180
SC	0.80	5.0	0.05	0.20	0.50	1.00	360

The functionality profile is evaluated based on traffic flow analysis. For a highway network with two or three bridges and five damage states, the possible network functionality profiles are 5^2=25 and 5^3=125, respectively. The corresponding resilience values are reported in matrix form in Table 4 for network N1 and in Tables from 5 to 9 for network N2, for increasing damage levels of bridge B_3. The most critical bridge in terms of system functionality and resilience is B_1, which is farther than bridge B_2 from the re-entry link. In addition, the network upgrade enhances the redundancy of the system, leading to higher levels of resilience. However, its effect progressively decreases as the damage state of bridge B_3 increases, reducing in this way the beneficial effect of traffic flows rerouted to the new highway branch introduced by the upgrade in the road infrastructure pattern.

Table 4. Resilience matrix of highway network N1.

B_1 \ B_2	No damage	SD	MD	ED	SC
No damage	1.000	0.990	0.958	0.806	0.507
SD	0.978	0.973	0.945	0.806	0.507
MD	0.925	0.921	0.907	0.800	0.506
ED	0.737	0.737	0.736	0.715	0.479
SC	0.380	0.380	0.380	0.376	0.340

Table 5. Resilience matrix of highway network N2 assuming no damage on bridge B_3.

B_1 \ B_2	No damage	SD	MD	ED	SC
No damage	1.000	0.998	0.985	0.922	0.786
SD	0.998	0.997	0.984	0.922	0.786
MD	0.985	0.984	0.979	0.921	0.786
ED	0.922	0.922	0.921	0.917	0.786
SC	0.786	0.786	0.786	0.786	0.778

Table 6. Resilience matrix of highway network N2 assuming bridge B_3 at SD limit state.

B_1 \ B_2	No damage	SD	MD	ED	SC
No damage	1.000	0.990	0.979	0.919	0.784
SD	0.977	0.973	0.963	0.909	0.774
MD	0.967	0.963	0.960	0.908	0.774
ED	0.911	0.909	0.908	0.904	0.774
SC	0.777	0.774	0.774	0.774	0.766

Table 7. Resilience matrix of highway network N2 assuming bridge B_3 at MD limit state.

B_1 \ B_2	No damage	SD	MD	ED	SC
No damage	1.000	0.990	0.963	0.910	0.776
SD	0.978	0.973	0.947	0.900	0.767
MD	0.928	0.924	0.913	0.877	0.747
ED	0.886	0.883	0.877	0.873	0.747
SC	0.754	0.752	0.747	0.747	0.739

Table 8. Resilience matrix of highway network N2 assuming bridge B_3 at ED limit state.

B_1 \ B_2	No damage	SD	MD	ED	SC
No damage	1.000	0.990	0.961	0.809	0.698
SD	0.978	0.973	0.947	0.808	0.698
MD	0.927	0.923	0.911	0.803	0.694
ED	0.740	0.739	0.738	0.718	0.629
SC	0.643	0.643	0.642	0.629	0.621

Table 9. Resilience matrix of highway network N2 assuming bridge B_3 at SC limit state.

B_1 \ B_2	No damage	SD	MD	ED	SC
No damage	1.000	0.990	0.958	0.806	0.512
SD	0.978	0.973	0.945	0.806	0.512
MD	0.925	0.921	0.907	0.800	0.511
ED	0.737	0.737	0.736	0.715	0.483
SC	0.383	0.383	0.383	0.379	0.347

Earthquake scenarios and life-cycle seismic resilience of the highway networks

Figure 4 shows the relationship between the PGA [g] versus epicentral distance *d* for different values of the moment magnitude *M* = 5.0, 5.5, 6.0, 6.5, 7.0, assuming soil type B of Eurocode 8 and reverse faulting, with site amplification F_S=0.162 and style-of-faulting correction F_{sof}=0.105 (Bindi *et al*. 2011).

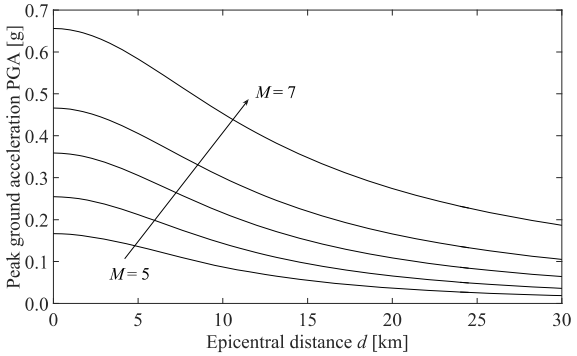

Figure 4. PGA [g] vs epicentral distance *d* for a moment magnitude *M*= 5.0, 5.5, 6.0, 6.5, 7.0.

Each bridge in the network is exposed to a different seismic demand depending on the magnitude and epicentral distance. The influence of the earthquake scenario on the time-variant seismic performance of the bridges is investigated by considering a grid of potential epicenters with size 1×1 km, as shown in Figure 5, and a magnitude *M*=7. Furthermore, the effectiveness of an infrastructural investment through the construction of a new highway with an additional bridge is evaluated by means of a life-cycle seismic resilience assessment of the road network. Five different scenarios are considered. In the first scenario, the network N1 with no upgrading is evaluated. In the other four scenarios, the network N1 is upgraded to network N2 with the new road branch added after *t*=100, 75, 50 and 25 years.

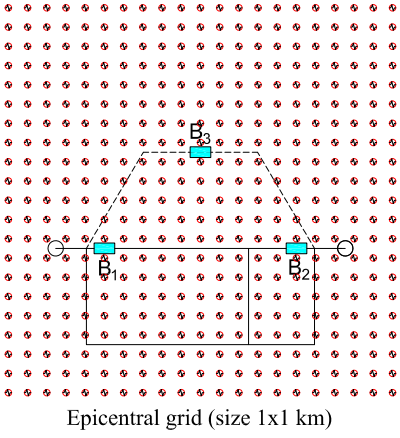

Figure 5. Grid of potential epicenters for the earthquake scenarios (grid size 1×1 km).

The contour maps shown in Figure 6 clearly indicate that resilience decreases over time due to the detrimental effects of structural deterioration. The impact of the environmental exposure depends on the earthquake scenario and related seismic exposure of the most important bridges in the network. From "year 0" to "year 50" the drop of seismic resilience is higher when the epicenter is closer to the most important bridge in the network (bridge B_1). At "year 100", the resilience contour map tends to flatten between the two bridges, approaching the minimum value when both bridges reach the SC limit state.

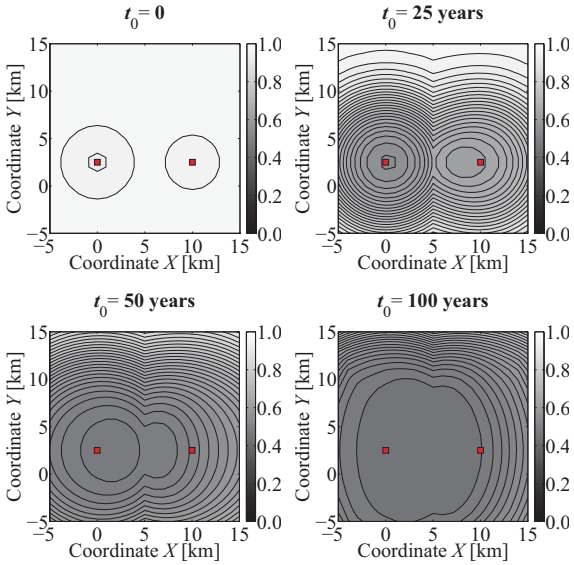

Figure 6. Lifetime resilience contour maps versus the epicenter location for network N1 for magnitude *M*=7 and time of occurrence t_0=0, 25, 50 and 100 years (square dots represent the location of the bridges).

In order to model the aging process affecting the additional road branch in network N2, the lifetime fragility curves of bridge B_3 are considered with a proper shift in time associated with the year at which the new highway is built. The resilience contour maps are shown in Figure 7. It is noted that the upgrading always involves an increase of seismic resilience over time. However, the beneficial effects of the upgrading are more important when bridges B_1 and B_2 exhibit moderate to severe damage states, making the new highway effective even for high seismic demand. This emphasizes the key role of the mutual influence among earthquake scenario, location of vulnerable structures and system management interventions in a multi-hazard life-cycle-oriented approach to seismic design of resilient structures and infrastructure systems.

For the purpose of the presented application, identical bridges with fully correlated fragility curves have been assumed. However, it is worth noting that different bridges and different levels of correlation can be easily accommodated in the proposed framework.

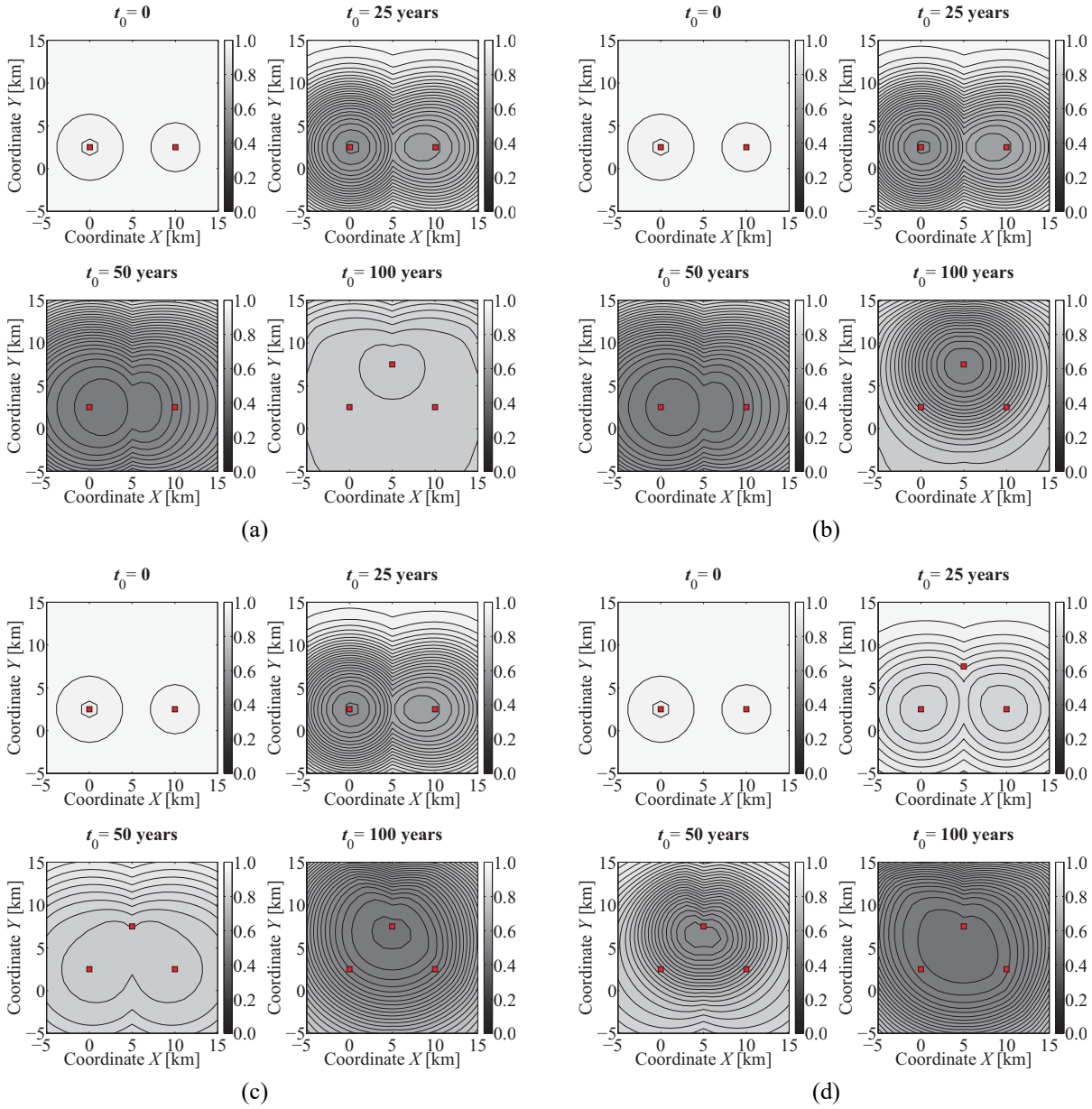

Figure 7. Lifetime resilience contour maps versus the epicenter location for network N2 for magnitude M=7 and time of occurrence t_0=0, 25, 50 and 100 years, considering the network upgrading after (a) 100 years, (b) 75 years, (c) 50 years, and (d) 25 years (square dots represent the location of the bridges).

Conclusions

A life-cycle probabilistic approach to seismic assessment of bridge structures and resilience analysis of road networks has been presented and applied to highway networks with RC bridges exposed to chloride-induced corrosion. An upgrade of an existing network by introducing a new highway branch at different time intervals during the service life of the system has been considered within a proper road management perspective. A parametric analysis has been carried out by varying the epicenter location to investigate the influence of the earthquake scenario and the role of bridge location in the network layout.

The results showed that the effects of aging and structural deterioration can significantly reduce over time the seismic capacity of bridges. Moreover, the increase in functionality of the highway system due to network upgrade always leads to an overall increase of seismic resilience at any time. Based on these results, a multi-hazard life-cycle-oriented approach to seismic design of resilient structures and infrastructure systems must consider the interdependency among several factors, such as seismic hazard, vulnerability of each structure depending on geographic location within the network, and structural recovery interventions carried out to restore the pre-event network functionality.

Further research is necessary for a more complete understanding of the processes involved in the earthquake-induced disruption of road networks and communities and their effective and prompt recovery. More specifically, additional considerations should be made upon the geographic layout of the bridges in the network, their mutual correlations, and how they affect the network seismic performance. Moreover, it is important to account for the mutual interaction of different hazards related to earthquakes, such as landslides, site amplification effects, liquefaction and cumulative damage induced by mainshock-aftershock sequences, among others.

References

Bertolini, L., Elsener, B., Pedeferri, P. and Polder, R. 2004. *Corrosion of steel in concrete*. Wiley-VCH, Weinheim, Germany.

Bindi, D., Pacor, F., Luzi, L., Puglia, R., Massa, M., Ameri, G. and Paolucci, R. 2011. Ground motion prediction equations derived from the Italian strong motion database. *Bulletin of Earthquake Engineering*, 9(6), 1899-1920.

Biondini, F., Bontempi, F., Frangopol, D.M. and Malerba, P.G. 2004. Cellular automata approach to durability analysis of concrete structures in aggressive environments. *Journal of Structural Engineering*, ASCE, 130(11), 1724-1737.

Biondini, F., Bontempi, F., Frangopol, D.M. and Malerba, P.G. 2006. Probabilistic service life assessment and maintenance planning of concrete structures. *Journal of Structural Engineering*, ASCE, 132(5), 810-825.

Biondini, F., Camnasio, E. and Titi, A. 2015a. Seismic resilience of concrete structures under corrosion. *Earthquake Engineering & Structural Dynamics*, 44(14), 2445-2466.

Biondini, F., Capacci, L. and Titi, A. 2015b. Seismic resilience of bridges and highway networks. *16th Congress of the Italian Association of Earthquake Engineering* (ANIDIS 2015), L'Aquila, Italy, September 13-17, 2015.

Biondini, F., Capacci, L. and Titi, A. 2016. Seismic resilience of aging bridges and transportation networks. *8th International Conference on Bridge Maintenance, Safety and Management* (IABMAS 2016), Foz do Iguaçu, Brazil, June 26-30, 2016. In: *Maintenance, Monitoring, Safety, Risk and Resilience of Bridges and Bridge Networks*, T. Bittencourt, D.M. Frangopol and A.T. Beck (Eds.), CRC Press/Balkema, Taylor and Francis, London, UK.

Biondini, F., Capacci, L. and Titi, A. 2017. Life-cycle resilience of deteriorating bridge networks under earthquake scenarios. 1*6th World Conference on Earthquake Engineering* (16th WCEE), Santiago, Chile, January 9-13, 2017.

Biondini, F. and Vergani, M. 2015. Deteriorating beam finite element for nonlinear analysis of concrete structures under corrosion. *Structure and Infrastructure Engineering*, 11(4), 519-532.

Bocchini, P. and Frangopol, D.M. 2011. A stochastic computational framework for the joint transportation network fragility analysis and traffic flow distribution under extreme events. *Probabilistic Engineering Mechanics*, 26(2), 182-193.

Bocchini, P. and Frangopol, D.M. 2012. Optimal resilience- and cost-based post-disaster intervention prioritization for bridges along a highway segment. *Journal of Bridge Engineering*, ASCE, 17(1), 117-129.

Bruneau, M., Chang, S.E., Eguchi, R.T., Lee, G.C., O'Rourke, T.D., Reinhorn, A.M., Shinozuka, M., Tierney, K., Wallace, W.A. and Winterfeldt, D.V. 2003. A framework to quantitatively assess and enhance the seismic resilience of communities. *Earthquake Spectra*, 19(4), 733-752.

Bruneau, M. and Reinhorn, A.M. 2007. Exploring the concept of seismic resilience for acute care facilities. *Earthquake Spectra*, 23(1), 41-62.

Capacci, L. 2015. *Seismic resilience of bridge networks*. Master Thesis, Politecnico di Milano, Milan, Italy.

Carturan, F., Pellegrino, C., Rossi, R., Gastaldi, M. and Modena, C. 2013. An integrated procedure for management of bridge networks in seismic areas. *Bulletin of Earthquake Engineering*, 11(2), 543-559.

CEN-EN 1998-1 2004. *Eurocode 8: Design of structures for earthquake resistance – Part 1: General rules, seismic actions and rules for buildings*. European Committee for Standardization, Brussels, Belgium.

Chang, S.E. 2009. Infrastructure resilience to disasters. *Frontiers of Engineering*, 39(4), 36-41.

Chang, S.E. and Shinozuka, M. 2004. Measuring improvements in the disaster resilience of communities. *Earthquake Spectra*, 20(3), 739-755.

Cimellaro, G.P., Reinhorn, A.M. and Bruneau, M. 2010. Framework for analytical quantification of disaster resilience. *Engineering Structures*, 32(11), 3639-3649.

Decò, A., Bocchini, P. and Frangopol, D.M. 2013. A probabilistic approach for the prediction of seismic resilience of bridges. *Earthquake Engineering & Structural Dynamics*, 42(10), 1469-1487.

Dolšek, M. 2009. Incremental dynamic analysis with consideration of modeling uncertainties. *Earthquake Engineering & Structural Dynamics,* 38(6), 808-825.

Mackie, K.R. and Stojadinović, B. 2006. Post-earthquake functionality of highway overpass bridges. *Earthquake Engineering & Structural Dynamics*, 35(1), 77-93.

Mander, J.B., Dhakal, R.P., Mashiko, N. and Solberg, K.M. 2007. Incremental dynamic analysis applied to seismic financial risk assessment of bridges. *Engineering Structures*, 29(10), 2662-2672.

Mander, J., Priestley, M.J.N. and Park, R. 1988. Theoretical stress-strain model for confined concrete. *Journal of Structural Engineering*, 114(8), 1804-1826.

Martin, W.A. and McGuckin, N.A. 1998. *Travel estimation techniques for urban planning*. NCHRP Report 365, Transportation Research Board, TRB, Washington, DC, USA.

Padgett, J.E. and DesRoches, R. 2007. Bridge functionality relationships for improved seismic risk assessment of transportation networks. *Earthquake Spectra*, 23(1), 115-130.

Papageorgiou, G., Mouratidis, A. and Eliou, N. 2012. Comprehensive model for upgrading two-lane road network. *European Transport Research Review*, 4(3), 125-135.

Paulay, T. and Priestley, M.J.N. 1992. *Seismic design of reinforced concrete and masonry structures*, John Wiley and Sons, Hoboken, NJ, USA.

SIMQKE 1976. *A program for artificial ground motion generation*. User's Manual and Documentation, NISEE, Massachusetts Institute of Technology, MA, USA.

Takeda, T., Sozen, M.A. and Nielsen, N.N. 1970. Reinforced concrete response to simulated earthquake. *Journal of the Structural Division*, ASCE, 11(2), 10-21.

Titi, A. and Biondini, F. 2013. Resilience of concrete frame structures under corrosion. *11th International Conference on Structural, Safety and Reliability* (ICOSSAR 2013), New York, NY, USA, June 16-20. In: *Safety, Reliability, Risk and Life-Cycle Performance of Structures and Infrastructures*, G. Deodatis, B.R. Ellingwood and D.M. Frangopol (Eds.), CRC Press/Balkema, Taylor and Francis Group, London, UK.

Titi, A., Biondini, F. and Frangopol, D.M. 2015. Seismic resilience of deteriorating concrete structures, *Proceedings of the ASCE Structures Congress*, Portland, OR, USA, April 22-25, 2015. In: *Structures Congress 2015*, N. Ingraffea and M. Libby (Eds.), ASCE, CD-ROM, 1649-1660.

Vamvatsikos, D. and Cornell, C.A. 2002. Incremental dynamic analysis. *Earthquake Engineering & Structural Dynamics*, 31(3), 491-514.

Venkittaraman, A. and Banerjee, S. 2014. Enhancing resilience of highway bridges through seismic retrofit. *Earthquake Engineering & Structural Dynamics*, 43(8), 1173-1191.